Three-Dimensional Analysis of Bone Formation After Maxillary Sinus Augmentation by Means of Microcomputed Tomography: A Pilot Study

Sebastian Kühl, Dr Med Dent[1]/Hermann Götz, Dipl Phys[2]/Torsten Hansen, Dr Med Habil[3]/Matthias Kreisler, Prof Dr Med Dent[4]/Alexandra Behneke, Priv Doz Dr Med Dent[5]/Uli Heil, Dipl Inf[6]/Heinz Duschner, Univ Prof Dr[7]/Berndt d'Hoedt, Univ Prof Dr Med Dent[8]

Purpose: *Although many studies have analyzed the suitability of different grafting materials for maxillary sinus augmentation by means of histomorphometry in conventional histologic strains, the three-dimensional (3D) structure and remodeling of these grafts after healing beneath the sinus membrane remain unclear. The aim of the present study was to determine whether microcomputed tomography is a suitable method to evaluate the 3D structure and remodeling of grafts after sinus floor augmentation.* ***Materials and Methods:*** *Sinus floor augmentation was performed in five patients using autogenous bone (AB) alone, AB and beta-tricalcium phosphate (β-TCP, Cerasorb), AB and β TCP/hydroxyapatite (HA) (BoneCeramic), AB and calcium carbonate (Algipore), and AB and HA (PepGen). Specimens from the grafted sites were harvested by means of a trephine bur 5 to 16 months after maxillary sinus augmentation. Microcomputed tomography of these specimens was performed with a nominal isotropic resolution of 6 × 6 × 6 μm² voxel size. After segmentation, 3D images were reconstructed, and the distribution of bone and substitute material was evaluated by means of volumetric and density measurements.* ***Results:*** *In all images, both bone and substitute material could clearly be identified. The connectivity of trabeculae surrounding the substitute material was visible in the 3D reconstructions. Volumetric evaluation such as total bone volume, volume of substitute material, and trabecular thickness and spacing revealed differences between the different grafting materials.* ***Conclusion:*** *Microcomputed tomography is a promising method to evaluate the 3D structure of grafts after sinus floor augmentation with autogenous bone and bone substitute materials.* Int J Oral Maxillofac Implants 2010;25:930–938

Key words: *bone grafting, maxillary sinus augmentation, microcomputed tomography*

[1]Assistant Lecturer and Researcher, Clinic for Oral Surgery, Radiology, and Oral Medicine, University Hospital Basel, Switzerland; Department of Oral Surgery, Oral Radiology and Oral Medicine, Johannes Gutenberg-University of Mainz, Germany.
[2]Senior Researcher, Institute of Applied Structure and Microanalysis, Johannes Gutenberg University of Mainz, Germany.
[3]Lecturer and Researcher, Institute of Pathologie, Johannes Gutenberg University of Mainz, Germany.
[4]Professor and Lecturer, Praxisklinik for Oral Surgery and Implantology, Germany; Department of Oral Surgery, Oral Radiology and Oral Medicine, Johannes Gutenberg University of Mainz.
[5]Lecturer, Clinic for Oral Surgery, Radiology, and Oral Medicine, University Hospital Basel, Switzerland; Department of Oral Surgery, Oral Radiology and Oral Medicine, Johannes Gutenberg-University of Mainz, Germany.
[6]Assistant Lecturer and Researcher, Institute for Informatics, Johannes Gutenberg University of Mainz, Germany.
[7]Leader of the Institute of Applied Structure and Microanalysis, University Medical Center of the Johannes Gutenberg University.
[8]Professor and Chair, Department of Oral Surgery, University Medical Center of the Johannes Gutenberg-University of Mainz.

Correspondence to: Dr Sebastian Kühl, Department of Oral Surgery, Oral Radiology, Oral Medicine, Hebelstrasse 3, 4056 Basel, Switzerland. Fax: +41-61-2672607. Email: dr.kuehl@email.de

Sinus elevation, as first described by Boyne and James[1] or modified by Tatum,[2] has proven to be a successful means to rehabilitate the atrophic posterior maxilla in conjunction with dental implants.[3–10] A variety of materials is recommended for external sinus lifts. Autologous bone, usually taken from the oral cavity or iliac crest, remains the gold standard.[11,12] Substitute materials have become popular because of their low postoperative morbidity, the unlimited amount of available material, and the time savings that result from omitting the donor site operation.[13,14] Irrespective of the material or technique applied, it is vital to obtain knowledge about the structural changes within the graft following maxillary sinus augmentation, especially because functional loading follows implant insertion. The most appropriate material for maxillary sinus augmentation is still a subject of controversy.[15,16]

Structural changes that occur during the healing of different grafting materials have been described and analyzed by means of histology and histomorphometry in both human and animal studies.[3,4,14,17–20]

Copyright by Not for Publication Presence

The authors used bony cylinders, which were obtained with a trephine bur from the augmented area at time of implant insertion. In most cases, the specimens were histologically sectioned according to the protocol of Donath and Breuner.[21] After staining with toluidine blue and basic fuchsin, morphometric measurements, such as total bone volume, the volume of bone substitute material, the bone-to-substitute contact area, the volume of the bone marrow, the volume of soft tissue, and other parameters, can be determined according to the protocol of Parfit et al.[22] Apart from morphometric analysis, the histologic process allows for evaluation of the number and type of different cells.[23] Although histomorphometric evaluation provides much information, it still represents only the two-dimensional structure of a material that is three-dimensional (3D) in nature. The biomechanical properties of a graft can only be evaluated by knowledge of its 3D structure. Based on stereology, the third dimension can be calculated from two-dimensional histologic strains; however, this procedure is tedious and time consuming.[24]

Microcomputed tomography (μCT) is a nondestructive radiographic procedure that provides 3D radiographs of hard tissues with a spatial resolution of up to $6 \times 6 \times 6$ μm^2. Since μCT has been used successfully to characterize the 3D structure of bone with morphometric precision comparable to that of classic histomorphometry, the question arises whether μCT is also suitable for evaluation of the remodeling of bone substitute material after healing in the human jaw.

The aim of the present study was to determine whether μCT is suitable to assess 3D radiographs of different grafted materials at the time of implant insertion after maxillary sinus augmentation. In addition to the visual perception of the bone and substitute material, a determination of the bone/substitute material volume ratio was performed for five different materials: autologous bone (AB) alone, AB and beta-tricalcium phosphate, AB and a mixture of hydroxyapatite (HA) and β-TCP, AB and calcium carbonate, and AB and HA.

MATERIALS AND METHODS

Patients

The study protocol was approved by the ethics committee of Johannes Gutenberg University of Mainz (Nr. 837.158.08 [6155]). Five healthy patients (two men, three women, ages 38 to 61 years) who had undergone maxillary sinus augmentation procedures were included in this study and signed a consent form.

Table 1 Clinical Data of Patients Studied

Patients	Age*	Sex	Graft material	Healing period (mo)
A	38	F	Bone (block) linea obliqua	7
B	61	M	Autogenous bone + Cerasorb	7
C	51	F	Symphysis + BoneCeramic	5
D	53	F	Linea obliqua + Algipore	14
E	61	F	Linea obliqua + CeraMed	16

*In years, at the time of sinus augmentation.

Surgical Procedure

A mucoperiosteal flap was elevated, and access to the sinus membrane was obtained by drilling an oval hollow into the facial sinus wall with a thick dental bur. The bone in the center of the created window was gently infractured and the intact sinus membrane was elevated. Once the sinus membrane was completely movable, the infractured bone was folded inward and upward, imitating a trap-door effect. Perforation of the sinus membrane occurred in one site (patient A).

AB, which was harvested as a block either from the mandibular symphysis or the linea obliqua of the mandible, was particulated using a surgical bone mill (Quetin Bone Mill, Quetin Dental Products), except for patient A. In patient A, as the result of a perforation of the sinus membrane, the bone block was fixed with two osseosynthetic screws (Synthes). In the other patients, the particulated bone was mixed with blood taken from the donor site, and substitute material was added to the particulated bone in a ratio of approximately 50%. In patient B, β-TCP (Cerasorb 1,000 to 2,000 μm, Curasan) was used; in patient C, a β-TCP/HA mixture (BoneCeramic 500 to 1,000 μm, Institut Straumann) was used; in patient D, calcium carbonate (Frios Algipore, Dentsply Friadent) was used; and in patient E, HA (Pepgen P-15, CeraMed Dental) was used (Table 1). In all patients, the window in the facial wall was closed by fixing a nonresorbable Gore-Tex membrane (WL Gore & Associates) with titanium nails (Frios, Dentsply Friadent).

Specimen Retrieval and Preparation

Bony cylinders were harvested from the grafted areas by means of a trephine bur with an internal diameter of 3.2 mm at the time of implant placement, 5 to 16 months after maxillary sinus augmentation (Table 1). The cylinders were gently removed from the trephine and immediately immersed in 4.5% buffered paraformaldehyde fixative (pH 7.0, Roti Histofix 4.5%; Carl Roth) for at least 7 days. After being dehydrated in alcohols of increasing concentrations, the cylinders were embedded in paraffin according to standard protocols (Hypercenter XP, Fa Shandon).

Copyright by

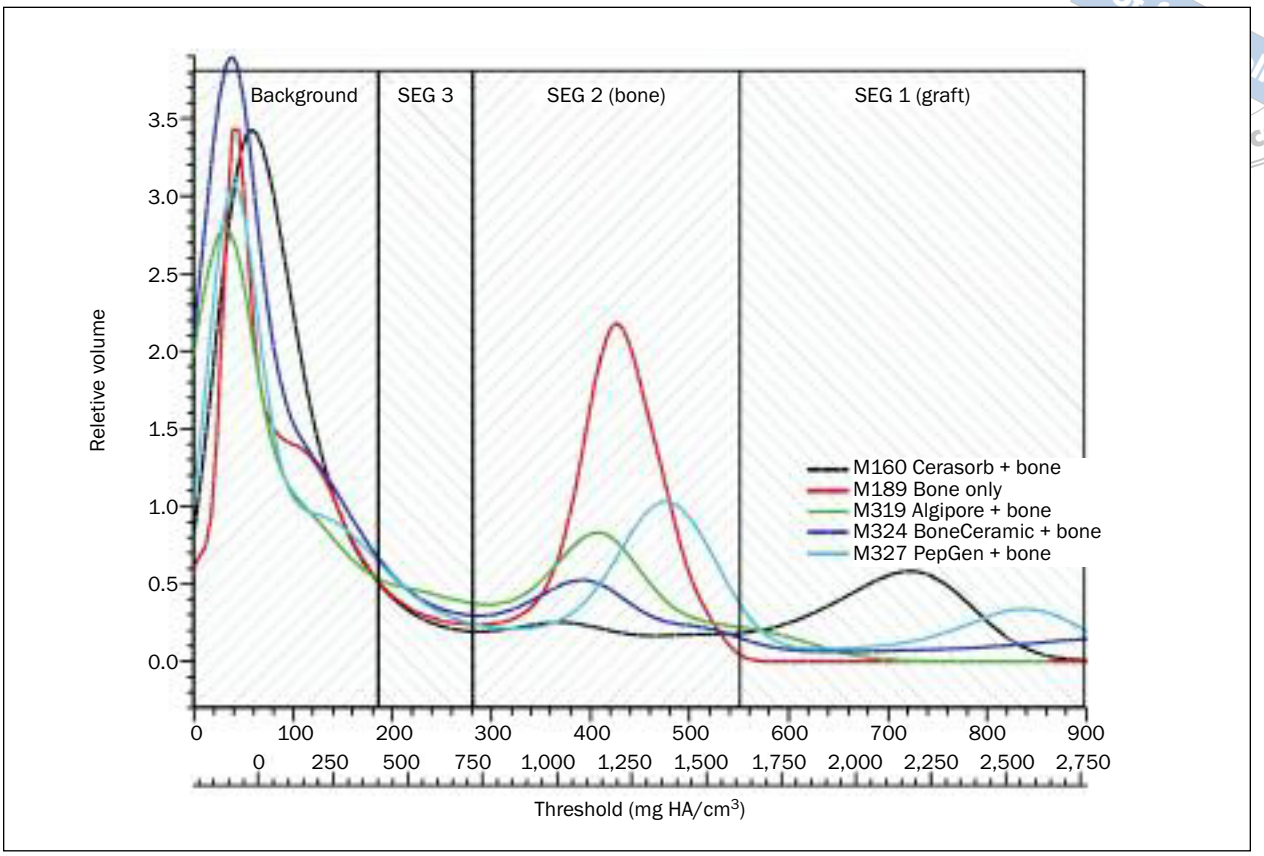

Fig 1 Grayscale histogram for each sample. Peaks below 280 represent soft tissue, peaks between 280 and 550 represent bone, and peaks over 550 represent the substitute material. The partial gray value histogram indicates equivalent density in mg HA/cm^3.

Radiography

The paraffin-embedded samples were then placed into pipettes of decreasing diameter (100 µL MBP Pipette Tips Nr. 3550, Molecular Bio-Products) so that they clamped as a result of their conus form. The pipettes were then fixed in a typical specimen holder (SCANCO Medical) for high-resolution µCT.

Radiography was performed with a cone-beam scanner (µCT-40, SCANCO Medical) in high-resolution mode with a nominal isotropic resolution of 6 µm. A microfocus x-ray source (70 kV, 113 µA) was used to produce the radiographs (0.18-degree angular increments, 300-ms integration time). Because of the mostly cylindric shape of the specimens, the height of the samples was the determining factor for the number of radiographs necessary to obtain tomographs with a voxel size of 6 µm. Typical acquisition times of 1 to 2 hours and 4,000 to 8,000 radiographs are necessary for the reconstruction of a cylindric sample of 6 to 12 mm in height. All calculations were carried out on two Hewlett-Packard 64-bit integrity servers simultaneously. For example, 2,000 µCT slices (2,048 × 2,048, 16-bit) are generated for the reconstruction of a sample that is 12 mm high.

Cross sections and longitudinal slices of the specimens were generated, and thresholds for the differentiation of bone and substitute material were obtained by means of a density parameter. The thresholds for bone and substitute material were placed at two different settings for segmentation of the pictures, based on the grayscale values and distribution in a histogram (Fig 1): SEG 1 = 550 to 1,000 greyscale values (representing high-density material, ie, the bone substitutes) and SEG 2 = 280 to 550 (representing intermediate-density material, ie, bone). The sample from patient A (bone) served as a reference, as it consisted only of bone. Following the segmentation process, a morphologic filter operation by means of dilatation and erosion in the border zones of the substitute materials was applied before evaluation with the Scanco imaging software to reduce artifacts. Three-dimensional reconstructions were performed using Scanco medical imaging software. Visual evaluation of the 3D images included determination and visibility of bone and substitute material, resorption, and bone apposition.

Copyright by

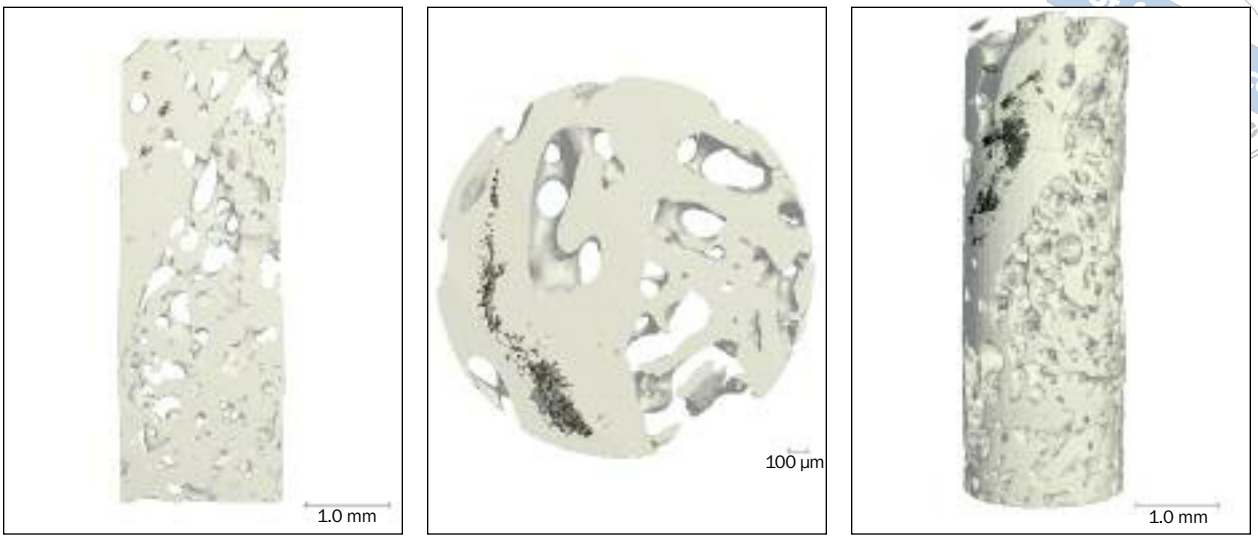

Fig 2 *(Left)* Longitudinal and *(center)* cross-sectional reconstructions after segmentation show compact bone *(grey)* with only small spaces. Because of the high density of the bone, the cross-sectional and *(right)* 3D reconstructions show some substitute material *(green)*, even though the graft consists only of bone.

Different parameters were examined for the quantitative evaluation of the sample structure. First, the total volume (TV) of interest was defined for every sample, which includes all soft tissue and hard tissue compounds. Within this volume, the volume of substitute material (VS) as a percentage was determined by setting the threshold at 550 to 1,000. The bone volume (BV) was also determined as a percentage by setting the threshold at 280 to 550. Furthermore, the specific volume of the substitute material (SpVS) was calculated as a percentage of the total hard tissue volume alone (VS/[VS + BV]). Mean density values (sample density) for both segments were calculated in mg HA/cm^3. Based on these parameters, morphometric evaluation was performed based on the protocol of Parfitt et al,[22] including trabecular thickness (TbTh) and trabecular separation (TbSp), which represents the space in between the hard tissues.

RESULTS

Table 1 provides information on the patients included in the study, including the healing time that elapsed prior to retrieval of graft specimens.

Cross-sectional and longitudinal radiographs of each sample clearly showed the bone and substitute material, which could easily be differentiated by their differing density and characteristic structure (Figs 2 to 6). The 3D reconstructions in Figs 2 to 6 show the stereoscopic architecture of the bone (grey) and the embedded substitute material (colored). Soft tissue parameters such as bone marrow or connective tissue are not visible in the radiographs.

The 3D reconstruction of sample A (AB) showed the typical structure of trabecular and cortical bone (Fig 2a), including a small area with reconstructed substitute material (Fig 2c). The space between the bone trabeculae was small (Fig 2b). In some regions the bone showed large trabeculae which appeared fairly flat. BV was 58.98% and the sample density was 1,194 mg HA/cm^3 (Table 2). Although no substitute material was used in this sample, the volumetric evaluation found 0.04% of substitute material at a mean density of 1,642 mg HA/cm^3 (Table 2). The SpVS of substitute material was calculated to be 0.07%. Mean TbSp was 204 µm (median = 186 µm) and mean TbTh was 236 µm (median = 186 µm) (Table 2).

Within specimen B (Cerasorb), three different zones could be detected (Fig 3): A first zone representing the typical structure of regional bone; a second zone with inhomogeneous, porous surfaces of the substitute material particle and interproximal trabecular structure; and a third zone in which the grafted material had a smooth surface without interproximal bony structure. The porous structure of the round substitute particles is clearly visible. BV was 11.56% with a mean sample density of 1,084 mg HA/cm^3. The volume of the substitute material was 16.95% and the density was 2,115 mg HA/cm^3, whereas the SpVS was 59.45% (Table 2). Mean TbSp was 323 µm (median = 300 µm) and the mean TbTh was 521 µm (median = 528 µm) (Table 2).

In sample C (Algipore), two different zones were detectable (Fig 4). At the bottom, the typical structure of trabecular bone was visible, which became more compact the closer it got to the substitute material. The space between the bone trabeculae was small

Copyright by

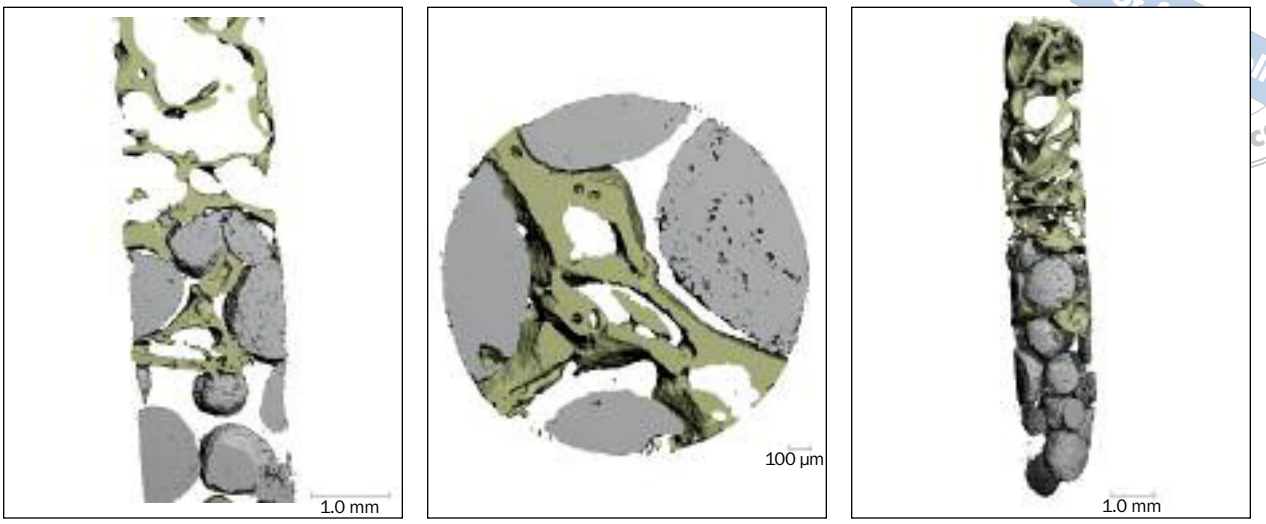

Fig 3 Bone *(green)* and substitute material (Cerasorb) *(grey)* are clearly visible in *(left)* the two-dimensional longitudinal, *(center)* cross-sectional, and *(right)* 3D reconstructions. The 3D reconstruction shows the three metabolic zones.

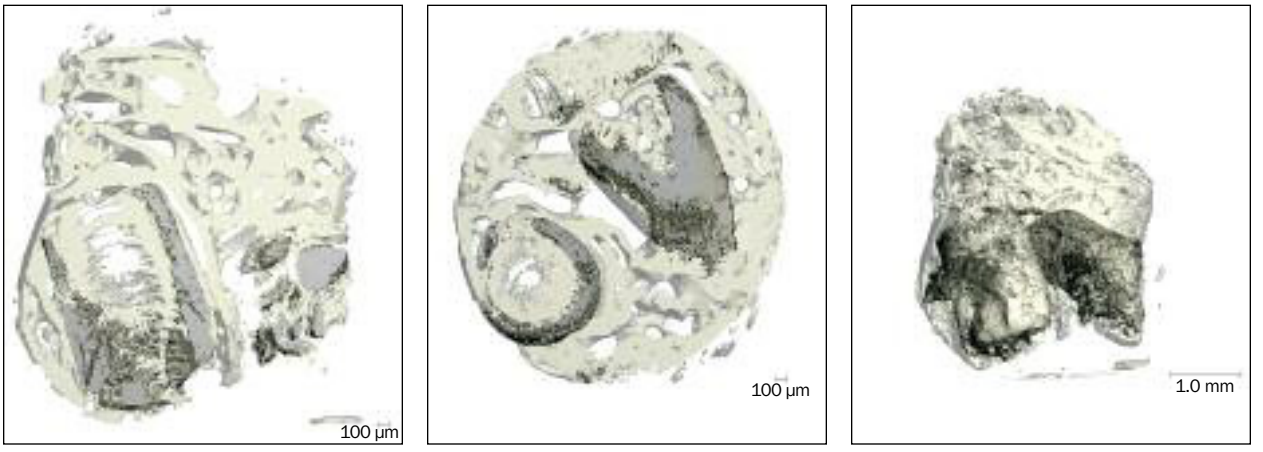

Fig 4 Bone *(grey)* and substitute material *(green)* (Algipore) is clearly visible in *(left)* longitudinal, *(center)* cross-sectional, and *(right)* 3D reconstructions after segmentation. The bone surrounding the substitute material has a very compact structure.

(Figs 4a and 4b) with a mean TbSp of 170 µm (median = 156 µm) and a mean TbTh of 201 µm (median = 150 µm) (Table 2). BV was 26.12% with a mean SD of 1,122 mg HA/cm^3. The substitute material had a BV of 3.59% and a mean sample density of 1,756 mg HA/cm^3 (Table 2). SpVS was calculated to be 12.05%.

The amount of visible substitute material from patient D (BoneCeramic) was greater and denser than in all other samples (Fig 5). The substitute material was mostly surrounded by bone and the substitute particles were sharp shaped. Volumetric evaluation revealed a BV of 18.61% at mean SD of 1,053 mg HA/cm^3. The substitute material had a BV of 10.43% with a mean sample density of 2,447 mg HA/cm^3 (Table 2). SpVS was calculated to be 35.98%, mean TbSp was 178 µm (median = 156 µm), and mean TbTh was 132 µm (median = 120 µm) (Table 2).

In the sample from patient E (PepGen), all particles were embedded in bone and the interproximal spaces were small. In comparison to the other substitute materials, the visible surface of the PepGen particles was greater (Fig 6). The borders of the substitute material particles were sharp. BV was 29.57% with a mean sample density of 1,227 mg HA/cm^3. The substitute material had a BV of 18.84% and a mean density of 2,331 mg HA/cm^3 with a SpVS of 38.92% (Table 2). For sample E, the morphometric evaluation revealed a mean TbSp of 159 µm (median = 138 µm) and a mean TbTh of 240 µm (median = 228 µm).

Copyright by

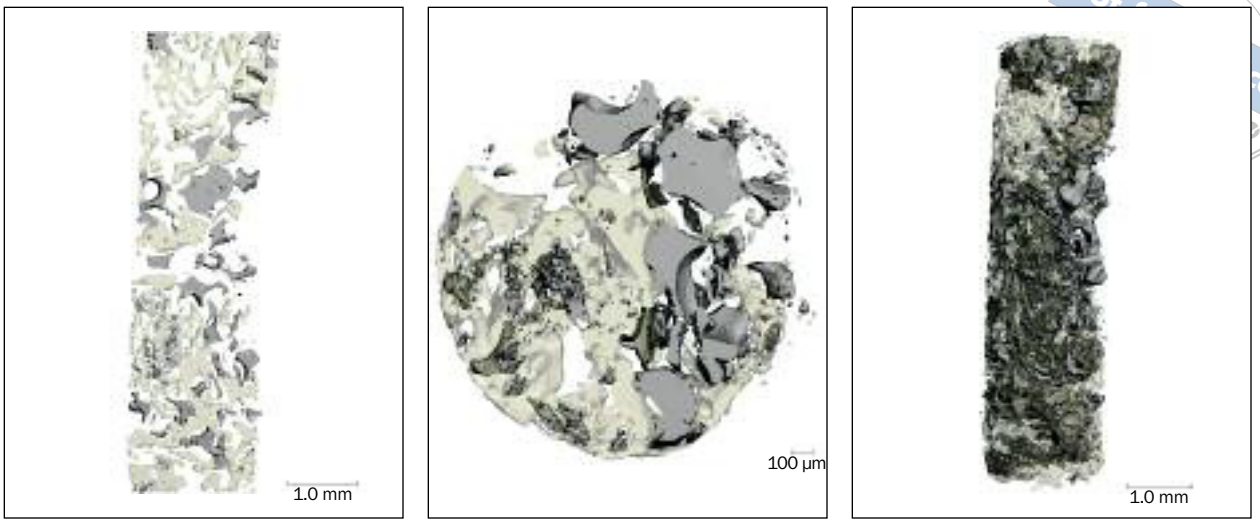

Fig 5 Bone *(green)* and substitute material *(grey)* (BoneCeramic) are clearly visible in *(left)* the longitudinal, *(center)* cross-sectional, and *(right)* 3D reconstructions after segmentation. The substitute material particles are sharp, with little space between the bone and substitute particles.

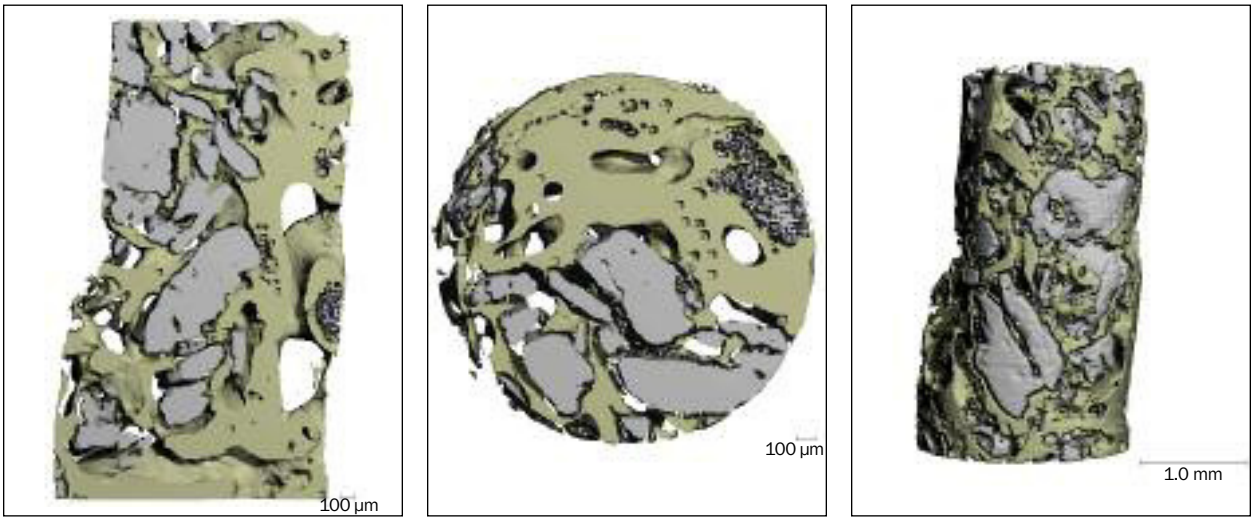

Fig 6 The substitute material (*grey*) (PepGen) is completely surrounded by bone (*green*) in (*left*) the longitudinal and (*right*) 3D reconstructions after segmentation. (*Center*) Only the cross-sectional reconstruction shows that some particles are partly without bony contact.

Table 2 Volumetric and Morphometric Evaluation of the Samples After Segmentation

	Sample A (bone)	Sample B (Cerasorb)	Sample C (Algipore)	Sample D (BoneCeramic)	Sample E (PepGen)
TV (mm^2)	24.86	53.16	49.41	30.05	14.97
VS (%)	0.04	16.95	3.58	4.17	18.84
VB (%)	58.98	11.56	26.12	32.65	29.57
SpVS (%)	0.07	59.45	12.05	11.33	38.92
SDB (mg HA/cm^3)	1,194	1,084	1,122	1,208	1,227
SDS (mg HA/cm^3)	—	2,115	1,756	2,339	2,331
TbSp (median)	204 (186)	323 (300)	170 (156)	178 (156)	159 (138)
TbTh (median)	236 (186)	521 (528)	201 (150)	132 (120)	240 (228)

TV = total volume (volume of interest. including soft tissue); VS = volume of substitute material within the TV; VB = volume of bone within TV; SpVS = specific volume of the substitute material within VS and VB (SpVS = VS/[VS+VB]); SDB = mean specific density of bone; SDS = mean specific density of substitute material; TbSp = mean (median) trabecular space in µm; TbTh = mean (median) trabecular thickness in µm.

Copyright by Quintessence Not for Publication

DISCUSSION

To understand the structural changes that take place after augmentation of the maxillary sinus with substitute materials, samples have been examined histologically.[14,15,18] Although histologic examination can reveal detailed information on the percentage distribution of tissue such as bone, substitute material, and soft tissue, as well as information on cellular components, it only provides information about the two-dimensional structure of the analyzed material. With regard to implant loading following grafting, it is vital to appreciate the 3D structure of healed grafts, as the stereologic structure determines the strength and characteristics of bony tissue.[25–27] Although maxillary sinus augmentation has shown a high predictability of success[3] and various bone substitute materials have been used successfully, it is not yet known which of these materials, except for AB, provides the greatest osteogenic potential and ideal biomechanical properties.[15]

Microcomputed tomography, which was first described by Feldkamp et al in 1989,[28] is a nondestructive, radiographic technique to assess 3D information about bony structures. In recent years, continuous development has made it possible to achieve images with a resolution of up to less than 10 μm^2 voxel size.[29,30] Thomsen et al[31] compared morphometric abilities of classical histology and μCT for cancellous bone and concluded that μCT could be used as a substitute for conventional histologic analysis for bone structural evaluation because of the high correlations of morphometric data evaluation.[31] Because μCT provides 3D images of hard tissues, the question arises as to whether it is also suitable to evaluate the morphometric structure of healed grafts containing bone and substitute materials.

In 2006, Trisi et al[32] compared μCT images with classical histologic samples of bone and substitute material after maxillary sinus augmentation with mixtures of bone and Biogran (Biomet 3i) in three patients. To the authors' knowledge, the present study is the first to describe and evaluate mixtures of particulated AB and Cerasorb, BoneCeramic, Algipore, or PepGen after maxillary sinus augmentation procedure using high-definition μCT. In agreement with the results reported by Trisi et al, the bone and substitute material were clearly distinguishable in all samples because of the lower density of the bone versus the substitute material. With regard to this, the bone values were all within a range of 1,084 mg HA/cm^3 and 1,227 mg HA/cm^3. The variations in the density of substitute material were greater, with the highest density seen for BoneCeramic (2,447 mg HA/cm^3) and the lowest for Algipore (1,756 mg HA/cm^3) owing to the different chemical and structural composition of the substitute materials. These differing densities made it possible to easily perform segmentation and assess parameters such as bone volume, the volume of the substitute material, and trabecular thickness, number, and space. The thicker the trabeculae are and the more trabeculae appear, the more bone seems to be able to resist biomechanical stress. The spacing stands in opposition to these parameters, as it depends directly on the proportion and number of trabeculae. The spacing might have a direct impact on the remodeling process, as it is well known that to ensure neovascularization and osteoconductivity for the regeneration of bony defects, spaces of about 200 to 400 μm are needed.[33,34]

As discussed by Trisi and coworkers,[32] it is difficult to observe newly formed bone because of the small difference in density versus the grafted particulated bone that was used in addition to the substitute material at time of grafting. In addition, all substitute material particles produced an artifact zone of approximate 5 μm in their vicinity. The evaluation of the bone volume or the volume of substitute material is strongly dependent on the threshold settings used for segmentation.[35] For example, in patient A, the reconstruction and evaluation showed that the sample consisted of 0.04% substitute material which corresponds to a specific volume of 0.07%, even though no substitute material was used in this sample. The reason for this can be found in the high density of the merely cortical structure of the bone, or perhaps in having set the threshold slightly too low for the substitute material. Interestingly, the present study generally used lower threshold settings than Trisi et al[32] for both bone and substitute material, which was defined in the present study after evaluating the histogram over all samples. Because the degree of mineralization of bone varies within individuals, a standardization of threshold settings for bone in general and for different substitute materials might cause difficulties. In any event, the density measurements for the bone in all other samples revealed grades comparable to that seen for sample A, even though a bony block was used in patient A and particulated bone was used in all others.

The volumetric distribution of bone varied strongly, from 58.98% for sample A to 11.56% for sample B (Cerasorb) (Table 2). Depending on the region in which the measurement is made, extreme differences can be observed. Specific volume with 59.45% of substitute material within the hard tissue volume is very high for Cerasorb and does not agree with the results of other histologic studies.[18,36,37] The high amount of remaining Cerasorb is astonishing, as it is the only substitute material used in this study that is asserted

Copyright by Quintessence Not for Publication

to be completely resorbable. The bone volume for sample C (BoneCeramic) and sample E (PepGen) is in agreement with volumetric measurements based on histologic specimens described in the literature, although the amount of substitute material in the current samples is much lower.[12,38] One reason for the high variability in the amount of remaining substitute material in the present samples could be variations in the mixture ratios of bone and substitute material estimated by the surgeon at time of maxillary sinus augmentation. The other reason could be the large differences in the healing periods, which ranged from 5 months for sample C (BoneCeramic) to 16 months for sample E (CeraMed). These large variations were unfortunately unavoidable and resulted in one delayed surgery. However, because this study focused on the evaluation of the suitability and abilities of µCT with regard to obtaining 3D information on the healing of four different substitute materials after sinus elevation and on the evaluation of the additional information that can be obtained compared to classical histologic examination, the differences in healing time as well as the small number of patients should not specifically affect the study's aim and conclusions.

The bone trabeculae surrounding the substitute material particles had a more compact structure than the local bone trabeculae. This could be a mineralizational effect induced by the substitute materials, as has been described in other studies.[39,40] In comparison to the study of Trisi and colleagues,[32] the mean TbSp and TbTh were generally much higher in the present study. This could be a result of the higher resolution (6 µm voxel size here, versus 20 µm used by Trisi et al). The low variation between means and medians in all samples shows that these data are reliable.

CONCLUSION

As shown in this study, three-dimensional reconstructions and morphometric evaluations are strongly dependent on the segmentation process that is performed. Therefore, conclusions should be made carefully with regard to volumetric evaluations. For better standardization and comparison of different strains, further studies are necessary to determine optimal threshold settings. The results of the present pilot study indicate that microcomputed tomography is a promising method to evaluate the three-dimensional structure of grafts after sinus floor augmentation with autogenous bone and bone substitute materials. A prospective study focusing on the healing of different substitute materials, which will be performed by microcomputed tomography with homogenous healing periods, is recommended.

ACKNOWLEDGMENT

This work is dedicated to Prof Dr Willi Schulte, who unfortunately passed away in December 2008.

REFERENCES

1. Boyne PJ, James RA. Grafting of the maxillary sinus floor with autogenous marrow bone. J Oral Surg 1980;38:613–616.
2. Tatum H. Maxillary and sinus implant reconstructions. Dent Clin North Am 1986;30:207–229.
3. Huerzeler MB, Kirsch A, Ackermann KL, Quinones CR. Reconstruction of the severely resorbed maxilla with dental implants in the augmented maxillary sinus: A 5-year clinical investigation. Int J Oral Maxillofac Implants 1996;11:466–475.
4. Huerzeler MB, Quinones CR, Kirsch A, et al. Maxillary sinus augmentation using different grafting materials and dental implants in monkeys. Part I. Evaluation of anorganic bovine-derived bone matrix. Clin Oral Implants Res Dec 1997;8: 476–486.
5. Quinones CR, Hurzeler MB, Schupbach P, et al. Maxillary sinus augmentation using different grafting materials and osseointegrated dental implants in monkeys. Part II. Evaluation of porous hydroxyapatite as a grafting material. Clin Oral Implants Res 1997;8:87–96.
6. Wallace S, Froum S. Effect of maxillary sinus augmentation on the survival of endosseous dental implants. A systematic review. Ann Periodontol 2003;8:328–343.
7. Szabo G, Huys L, Coulthard P, et al. A prospective multicenter randomized clinical trial of autogenous bone versus beta-tricalcium phosphate graft alone for bilateral sinus elevation: Histologic and histomorphometric evaluation. Int J Oral Maxillofac Implants 2005;20:371–381.
8. Kreisler M, Moritz O, Weihe CH, d'Hoedt B. Die externe Sinusbodenelevation vor dem Hintergrund der Evidenzbasierten Medizin, Teil I. Z Zahnärztl Implantol 2006;22:299–323.
9. Kreisler M, Moritz O, Weihe CH, d'Hoedt B. Die externe Sinusbodenelevation vor dem Hintergrund der Evidenzbasierten Medizin, Teil II. Z Zahnärztl Implantol 2007;23:68–86.
10. Peleg M, Garg AK, Mazor Z. Predictability of simultaneous implant placement in the severely atrophic posterior maxilla: A 9-year longitudinal experience study of 2132 implants placed into 731 human sinus grafts. Int J Oral Maxillofac Implants 2006;21:94–102.
11. Daelemans P, Hermans M, Godet F, Malevez C. Autologous bone graft to augment the maxillary sinus in conjunction with immediate endosseous implants: A retrospective study up to 5 years. Int J Periodontics Restorative Dent 1997;17:27–39.
12. Cordaro L, Bosshardt, Palattella P, Rao W, Serino G, Chiapasco M. Maxillary sinus grafting with Bio-Oss or Straumann bone ceramic: Histomorphometric results from a randomized controlled multicenter clinical trial. Clin Oral Implants Res 2008; 19:796–803.
13. Degidi M, Piattelli M, Scarano A, Iezzi G, Piattelli A. Maxillary sinus augmentation with a synthetic cell-binding peptide: Histological and histomorphometrical results in humans. J Oral Implantol 2004;30:376–383.
14. Artzi Z, Weinreb M, Carmeli G, Lev-Dor R, Dard M, Nemcovsky CE. Histomorphometric assessment of bone formation in sinus augmentation utilizing a combination of autogenous and hydroxyapatite/biphasic tricalcium phosphate graft materials: At 6 and 9 months in humans. Clin Oral Implants Res 2008;19: 686–692.

Copyright by Quintessence Not for Publication

15. Cordioli G, Mazzocco C, Schepers E, Brugnolo E, Majzoub Z. Maxillary sinus floor augmentation using bioactive glass granules and autogenous bone with simultaneous implant placement. Clin Oral Implants Res 2001;12:270–278.
16. Yildirim M, Spiekermann H, Biesterfeld S, Edelhoff D. Maxillary sinus augmentation using xenogenic bone substitute material Bio-Oss in combination with venous blood. A histologic and histomorphometric study in humans. Clin Oral Implants Res 2000;11:217–229.
17. Scarano A, Degidi M, Iezzi G, et al. Maxillary sinus augmentation with different biomaterials: A comparative histologic and histomorphometric study in man. Implant Dent 2006;15:197–207.
18. Artzi Z, Kozlovsky A, Nemcovsky CE, Weinreb M. The amount of newly formed bone in sinus grafting procedures depends on tissue depth as well as the type and resudual amount of the grafted material. J Clin Periodontol 2005;32:193–199.
19. Hallman M, Lundgren S, Sennerby L. Histologic analysis of clinical biopsies taken 6 months and 3 years after maxillary sinus floor augmentation with 80% bovine hydroxyapatite and 20% autogenous bone mixed with fibrin glue. Clin Implant Dent Relat Res 2001;3:87–96.
20. Huerzeler MB, Quinones CR, Kirsch A, et al. Maxillary sinus augmentation using different grafting materials and dental implants in monkeys. Part III. Evaluation of autogenous bone combined with porous hydroxyapatite. Clin Oral Implants Res 1997;8:401–411.
21. Donath K, Breuner G. A method for the study of undecalcified bones and teeth with attached soft tissues. The Säge-Schliff (sawing and grinding) technique. J Oral Pathol 1982;11:318–326.
22. Parfitt MA, Drezner MK, Glorieux FH, et al. Bone histomorphometry: Standardization of nomenclature, symbols, and units. J Bone Miner Res 1987;2:595–610.
23. Recker RR. Bone Histomorphometry: Technique and Interpretation. Boca Raton, FL: CRC, 1983.
24. Chappard D, Legrand E, Pascaretti C, Basle MF, Audran M. Comparison of eight histomorphometric methods for measuring trabecular bone architecture by image analysis on histological sections. Microsc Res Tech 1999;45:303–312.
25. Dalstra M, Huiskes R, Odgaard A, van Erning L. Mechanical and textural properties of pelvic trabecular bone. J Biomech 1993; 26:523–535.
26. Teo JC, Si-Hoe KM, Keh JE, et al. Relationship between CT intensity, micro-architecture and mechanical properties of porcine vertebral cancellous bone. Clin Biomech 2006;21:235–244.
27. Reynolds DG, Shaikh S, Papuga MO, et al. Micro-CT-based measurement of cortical bone graft-to-host union. J Bone Miner Res 2009;24:899–907.
28. Feldkamp LA, Goldstein SA, Parfitt AM, Jesion G, Kleerekoper M. The direct examination of three-dimensional bone architecture in vitro by computed tomography. J Bone Miner Res 1989;4:3–11.
29. Ito M. Assessment of bone quality using micro-computed tomography (micro-CT) and synchrotron micro-CT. J Bone Miner Metab 2005;23:115–121.
30. Rüegsegger P, Koller B, Müller R. A microtomographic system for the nondestructive evaluation of bone architecture. Calcif Tissue Int 1996;58:24–29.
31. Thomsen JS, Laib A, Koller B, Prohaska S, Mosekilde LI, Gowin W. Stereological measures of trabecular bone structure: Comparison of 3D micro computer tomography with 2D histological sections in human proximal tibial bone biopsies. J Microsc 2005;218:171–179.
32. Trisi P, Rebaudi A, Calcari F, et al. Sinus graft with Biogran, autogenous bone, and PRP: A report of three cases with histology and micro-CT. Int J Periodontics Restorative Dent 2006;26:113–125.
33. Chang BS, Lee CK, Hong KS, et al. Osteoconduction at porous hydroxyapatite with various pore configurations. Biomaterials 2000;21:1291–1298.
34. Karageorgius V, Kaplan D. Porosity of 3D biomaterial scaffolds and osteogenesis. Biomaterials 2005;26:5474–5491.
35. Freeman TA, Patel P, Parvizi J, Antoci V Jr, Shapiro IM. Micro-CT analysis with multiple thresholds allows detection of bone formation and resorption during ultrasound-treated fracture healing. J Orthop Res 2009;27:673–679.
36. Szuba Z, Takacs D, Matusovits D, Barabas J, Fazekas A, Szabo G. Maxillary sinus floor grafting with b-tricalcium phosphate in humans: Density and microarchitechture of the newly formed bone. Clin Oral Implants Res 2006;17:102–108.
37. Wiltfang J, Schlegel KA, Schultze-Mosgau S, Nkenke E, Zimmermann R, Kessler P. Sinus floor augmentation with b-tricalciumphosphate (ß-TCP): Does platelet-rich plasma promote its osseous integration and degradation? Clin Oral Implants Res 2003;14:213–218.
38. Froum SJ, Wallace SS, Cho SC, Elian N, Tarnow DP. Histomorphometric comparison of a biphasic bone ceramic to anorganic bovine bone for sinus augmentation: 6- to 8-month postsurgical assessment of vital bone formation. A pilot study. Int J Periodontics Restorative Dent 2008;28:273–281.
39. Gorustovic A, Rosenbusch M, Guglielmotto MB. Characterization of bone around titanium implants and bioactive glass particles: An experimental study in rats. Int J Oral Maxillofac Implants 2002;17:644–650.
40. Turunen T, Peltola J, Yli-Urpo A, Happonen R-P. Bioactive glass granules as a bone adjunctive material in maxillary sinus floor augmentation. Clin Oral Implants Res 2004;15:135–141.